Article:
Ramirez-Gutierrez, R, Zhang, LX and Elmirghani, J (2015) Antenna Beam Pattern Modulation with Lattice Reduction Aided Detection. IEEE Transactions on Vehicular Technology, PP (99). ISSN 0018-9545

https://doi.org/10.1109/TVT.2015.2422299

Antenna Beam Pattern Modulation with Lattice Reduction Aided Detection

Raymundo Ramirez-Gutierrez, Li Zhang and Jaafar Elmirghani

Abstract

This paper introduces a novel transmission design for antenna beam pattern modulation (ABPM) with a low complexity decoding method. The concept of ABPM was first presented with the optimal maximum likelihood (ML) decoding. However, an ML detector may not be viable for practical systems when the constellation size or the number of antennas is large such as in massive multiple input multiple output (MIMO) systems. Linear detectors, on the other hand, have lower complexity but inferior performance. In this paper, we present the antenna pattern selection with a lattice reduction (LR) aided linear detector for ABPM to reduce the detection complexity with the bit error rate (BER) performance approaching that of ML while conserving low complexity. Simulation results show that even with this suboptimal detection, performance gain is achieved by the proposed scheme compared to different spatial modulation techniques using ML detection. In addition, to validate the results, an upper bound expression for BER is provided for ABPM with ML detection.

I. Introduction

Wireless communications are constantly improving, providing an increased data rate, better quality of service and improved network capacity. Multiple input multiple output (MIMO) has shown extensive improvements over traditional single antenna systems. The most well known MIMO techniques are space-time coding (STC) [1] and spatial multiplexing [2] in cases where channel state information (CSI) is not available at the transmitter.

Submitted to *IEEE Trans. Veh. Technol.* in March 2014. This work was presented in part at the 2012 International Wireless Communications and Mobile Computer Conference, Cyprus 2012.

The authors are with the School of Electronic and Electrical Engineering, University of Leeds, Leeds LS2 9JT, United Kingdom (e-mail: ml07rr, l.x.zhang and j.m.h.elmirghani@leeds.ac.uk).

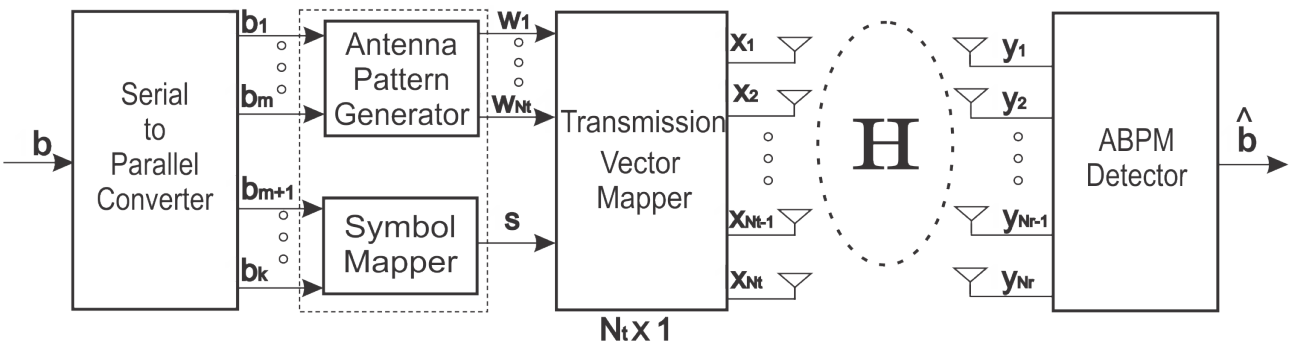

Fig. 1: ABPM system model.

STC aims to improve the reliability of the link which can be achieved by the transmission of multiple replicas of the same information through independent fading paths [1,2], reducing the probability that several signals fade at the same time.

Spatial multiplexing improves the spectral efficiency by transmitting multiple independent streams across multiple antennas. An example of such strategy is the vertical Bell Laboratories layered space-time (V-BLAST) architecture [3], which requires complex detection and equal or higher number of antennas at the receiver side compared to the transmitter side. Some hybrid encoding schemes have been suggested which increase diversity [4] and capacity [5] at the cost of increased computational complexity.

However, diverse constrains have been identified in the implementation of MIMO transmission schemes that have not been fully investigated [6,7], for instance:

- High inter-channel interference (ICI) is present at the receiver in BLAST transmission systems due to simultaneous transmissions from multiple antennas.
- The receiver algorithm complexity increases due to the presence of high ICI.
- Performance of BLAST schemes degrades significantly under non-ideal channel conditions [7].
- The above limitations are overcome with full diversity STCs [2,5]. But full-diversity STC systems (except Alamouti scheme) cannot achieve maximum spectral efficiency of one symbol per symbol duration. To achieve spectrum efficiency similar to that of BLAST techniques, full-diversity STCs need to use higher modulation schemes at the cost of reduced reliability.

Transmission techniques based on spatial modulation (SM) [8–12] have been proposed as a solution to dealing with these issues. They offer a simple design which achieves high data rate. In [13,14], generalized forms of SM were introduced. In these forms, combinations of antenna indices in addition to conventional M-ary modulation formats are used to convey the transmitted messages. In a scheme called generalized

phase spatial shift keying (GPSSK) modulation [14], the results show major improvement in terms of bit error rate (BER) over generalized space shift keying (GSSK) [12]. This improvement is the result of transmitting M-ary modulated signals instead of only energy at the position of the selected antennas. In this way, GPSSK improves spectrum efficiency compared with GSSK and SM without incurring extra detection complexity.

A beamspace-MIMO which maps phase-shift keying modulated symbols onto orthogonal basis functions on the wavevector domain of the multi-element antenna is proposed in [15–17]. Its performance is comparable to traditional MIMO systems although only a single active element is used for different beam patterns.

An antenna beam pattern modulation (ABPM) was proposed by the authors in [18]. ABPM shows a BER gain when compared to SM techniques employing an ML detector. It exploits the spatial channel using the antenna pattern to carry information to achieve an efficient information transmission. The beam pattern is determined by the antenna weights, based on the angle of departure (AoD) from the transmitter antenna array. All the techniques above use the optimal maximum likelihood (ML) as the optimal detector at the cost of high computation complexity, especially when the number of antennas and/or the constellation size are very large, such as in massive MIMO systems.

Linear detection schemes based on the zero forcing (ZF) or the minimum mean square error (MMSE) criteria are possible solutions [19] for lower complexity detection schemes. However, for ill-conditioned channels these techniques show an inferior performance compared to the ML detection. The concept of basis reduction was proposed more than a century ago [20] to find simultaneous rational approximations to real numbers and to solve the integer linear programming problem in fixed dimensions. The concept of lattice reduction (LR) is to find a reduced set of basis vectors for a given lattice to obtain certain properties such as short and nearly orthogonal vectors [20]. For this reason, the LR technique has recently been exploited to achieve a better conditioned channel matrix by improving its orthogonality conditions [21–25]. The Lenstra-Lenstra-Lovász (LLL) algorithm is widely used in LR to improve the performance of the linear detectors [26].

This article extends the work done in [18] by proposing optimal antenna pattern selection and reduced decoding complexity. To reduce the decoding complexity, this article proposes a suboptimal detection based on the LR technique and derives theoretical analysis for the scheme. The proposed scheme is evaluated by numerical simulation over independent and identically distributed (*i.i.d*) Rayleigh fading channel. The result proves feasible and shows improvements in both reliability and efficiency.

The rest of the article is organized as follows. Section II reviews the concept of ABPM and introduces

the transmission design, the selection of antenna beam pattern and the sub-optimal detection based on the LR scheme. Analytic calculation of BER is shown in Section III. Simulation results and comparisons with other transmission techniques follow in Section IV. The article is concluded in Section V.

Notation: Italicized symbols denote scalar values while bold lower denotes vectors and upper case symbols matrices. $(\cdot)^T$ and $(\cdot)^H$ for transpose and conjugate transpose respectively. $\|\cdot\|$ for the 2-norm of a vector/matrix is used and $\det(\cdot)$ indicates the matrix determinant. More notation used: $\mathcal{CN}(n, \sigma^2)$ for the complex Gaussian distribution of a random variable, with mean n and variance σ^2. I_N denotes the $N \times N$ identity matrix and $\mathbb{Z}$ is the integer set. $\mathcal{O}(\cdot)$ indicates the computational complexity in terms of number of arithmetic operations.

II. ABPM Description

The general ABPM system model consists of a MIMO wireless link between N_t transmit and N_r receive antennas. Fig. 1 illustrates the block diagram of ABPM. As shown in the figure, a random sequence of independent bits $\mathbf{b} = [b_1 \quad b_2 \quad \cdots \quad b_k]^T$ enters the serial to parallel converter. The first m bits select an antenna pattern and $k-m$ bits choose the conventional amplitude/phase modulation (APM) symbols. The output is mapped to a vector $\mathbf{x} = [x_1, \quad x_2, \quad \cdots, \quad x_{N_t}]^T$. The modulated signal is then transmitted over a $N_r \times N_t$ wireless channel $\mathbf{H}$. The received signal is given by $\mathbf{y} = \mathbf{Hx} + \mathbf{v}$, where $\mathbf{v} = [v_1 \quad v_2 \quad \cdots \quad v_{N_r}]^T$ represents the additive white Gaussian noise (AWGN) vector observed at the receive antennas with zero mean and covariance matrix $E[\mathbf{vv}^H] = \sigma_v^2 \boldsymbol{I_{Nr}}$. The channel matrix $\mathbf{H}$ has *i.i.d* entries with $\mathcal{CN}(0, 1)$. The channel is assumed to be flat-fading, time invariant and independently changing from symbol to symbol. In our system it is assumed that CSI is available at the transmitter (CSIT), such as in massive MIMO which is only feasible in reciprocal propagation channels as in time-division duplex (TDD) systems [27]. At the receiver, the antenna patterns and the APM symbol of the signals are estimated by the ABPM detector, and de-mapped to the transmitted bits.

A. ABPM Transmission

For each symbol period, a stream of independent bits $\mathbf{b}$ is sent to the serial to parallel converter and the output of the converter is divided into two blocks. The first m bits are used to indicate the antenna pattern which is realised by antenna weight vector denoted as $\mathbf{w} = [w_1, \quad w_2, \quad \cdots, \quad w_{N_t}]^T$. The second part of the symbol will determine the transmitted signal s on each antenna. The ABPM transmitted signal vector is a linear combination of s and $\mathbf{w}$, denoted as $\mathbf{x} = [w_1 \cdot s, \quad w_2 \cdot s, \quad \cdots, \quad w_{Nt} \cdot s]^T$.

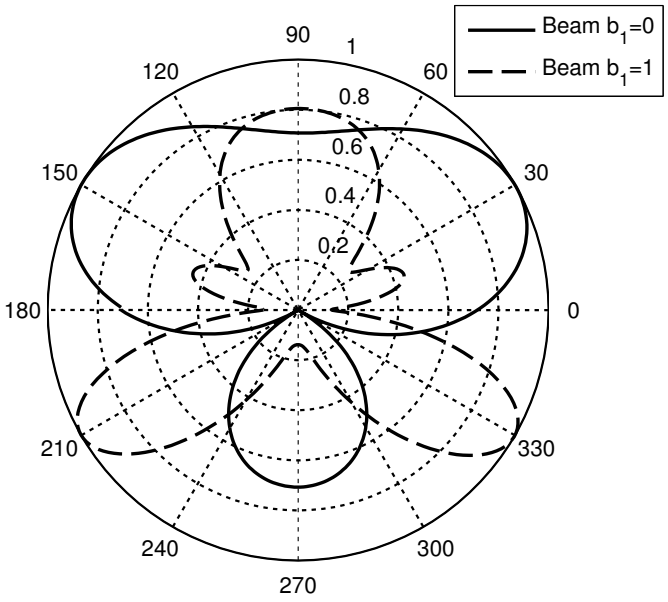

Fig. 2: The two possible beam patterns used in ABPM 2X4 with 3 bits/s/Hz.

The proposed ABPM is capable of transmitting symbols towards different AoDs at the transmitter side. Antenna patterns are realised by antenna weights, which can be selected to make the best channel utilisation possible by exploiting the CSIT. In order to facilitate the detection process, it is desirable for the selected patterns to have minimum correlation between them. The array response vector can be expressed as $\mathbf{a}(\theta) = [1 \quad e^{-i2\pi\frac{dsin\theta}{\lambda}} \quad \dots \quad e^{-i2\pi(N_t-1)\frac{dsin\theta}{\lambda}}]^T$, where d is the space between antenna elements, θ indicates the AoD and λ is the wavelength [28]. The distance between antenna elements has to be $d \geq \dfrac{\lambda}{2}$ to avoid correlation.

The weight vectors $\mathbf{w}$ should be obtained to satisfy $\mathbf{w}^H[\mathbf{a}(\theta_1) \ \ \mathbf{a}(\theta_2) \ \ \dots \ \ \mathbf{a}(\theta_{Nt})] = \mathbf{w}^H\mathbf{A} = [1, \ \cdots 0, \ \cdots 1, \ \ \cdots 0, \ \ \cdots 0]^T$. Note that, the "1" and "0" in this vector represents the main beam or nulls in the radiation pattern, respectively. In the case of where the steering of the main beam is wanted, "1" is selected. On the other hand, "0" is chosen when the pattern's nulls are desirable for design purposes. In this way, the beam patterns can be specified based on CSIT by the angles for the main beam and nulls. Clearly, as long as the number of independent columns in $\mathbf{A}$ is larger than N_t, $\mathbf{w}$ can be solved. So, we only included N_t columns in $\mathbf{A}$.

As mentioned in [18], the main contribution of this scheme is to use the antenna pattern to transmit symbol information, in addition to the conventional modulation symbols. ABPM transmits conventional

TABLE I: Correlation Table.

angle difference between main beam patterns	γ
10°	0.9281
20°	0.4885
30°	0.3536
40°	0.2953
50°	0.2679
60°	0.2556
70°	0.2511
80°	0.2503
90°	0.2493

TABLE II: Transmission Table of 2-ABPM System.

$[b_1$	b_2	$b_3]$	$Beam$	s
0	0	0	1	1 + i
0	0	1	1	1 - i
0	1	0	1	-1 - i
0	1	1	1	-1 + i
1	0	0	2	1 + i
1	0	1	2	1 - i
1	1	0	2	-1 - i
1	1	1	2	-1 + i

APM symbols by the selected beam patterns. We define the transmitted vector as $[w_1 \cdot s, \quad w_2 \cdot s, \quad \cdots, \quad w_{Nt} \cdot s]^T$ (i.e. ABPM symbol constellation points). Similar to traditional pulse-amplitude modulation (PAM), larger distance between two possible transmitted vectors will result in better performance. For ABPM, it is possible to maximize the distance between transmit vectors by choosing vectors with minimum correlation between them. The correlation between antenna beam patterns is denoted as γ with a range between 1 and 0, indicating completely correlated to no correlation, which is not always possible to achieve. Table I illustrates the correlation (γ) between two patterns (determined by AoD). A fixed angle is randomly selected (for simplicity and demonstrative purposes , 0° is selected as reference) and the other angle increments by 10°.

The 2^m antenna weight vectors $\mathbf{w}$ are combined with the APM symbol (selected by the second information block), to generate the transmit vector $\mathbf{x}$ which is transmitted over the channel. Thus the information is carried by both the beam pattern and the APM symbol through the channel $\mathbf{H}$. To clarify the transmission process an example is given below.

Each ABPM symbol carries 3 bits: two different beam patterns and QPSK modulation. The first block only has one bit and the second block contains two bits. The mapping table for 3 bits transmission using QPSK signal modulation and 2x4 MIMO antenna configuration is shown in Table II. The column 'beam' in Table II indicates which weight vector is selected at transmission, in other words which antenna beam pattern is used to transmit s. In this example, the beam patterns are: when $b_1 = 0$, the angle of the main beam is at 30° and the angle of the null is at -30° and when $b_1 = 1$, the angle of the main beam is at -30° and the angle of the null is at 0°.

Thus, the weight vectors can be calculated by

$$\mathbf{w}_1^H[\mathbf{a}(30^\circ) \;\; \mathbf{a}(-30^\circ)] = \begin{bmatrix} 1 \\ 0 \end{bmatrix} \qquad \mathbf{w}_2^H[\mathbf{a}(-30^\circ) \;\; \mathbf{a}(0^\circ)] = \begin{bmatrix} 1 \\ 0 \end{bmatrix}.$$

Solving the equations the weight vectors are: $\mathbf{w}_1 = [0.5000 + 0.0000i \quad 0.0000 - 0.5000i]^T$ and $\mathbf{w}_2 = [0.5000 - 0.5000i \quad -0.5000 + 0.5000i]^T$ and b_2 and b_3 are mapped to QPSK symbols according to Table II.

Fig. 2 shows both antenna beam patterns corresponding to $\mathbf{w}_1$ and $\mathbf{w}_2$ in the example above. The solid line shows the pattern corresponding to weight vector $\mathbf{w}_1$ in which the main beam is observed at 30° and the angle of the null at -30°. The dashed line represents the second pattern which has the main beam at -30° and the angle of the null at 0° to increase the directivity of the main lobe, corresponding to weight vector $\mathbf{w}_2$.

From Table I, it is concluded that the ABPM design for each of the 2^m patterns should have at least 20° separation in their main lobes to ensure a low correlation. Fig. 3 depicts the BER performance of ABPM based on different values of γ. The three curves are obtained under the same conditions: $N_t = 2$, $N_r = 4$, two beams patterns, QPSK symbols and the spectral efficiency (η) of 3 bits/s/Hz. The detection used for this figure is based on ML to demonstrate the impact of correlation on the selection of beam patterns. One of the beams was fixed to 0° and the second beam was selected based on Table I, to show the impact of different correlation values on the ABPM BER performance. The different angles selected are 60°, 20° and 10°. Each of these angles have a corresponding correlation value: $\gamma = 0.2556$, 0.4885 and 0.9281 respectively. It is shown that roughly 2 dB gain is obtained by low correlation patterns ($\gamma =$

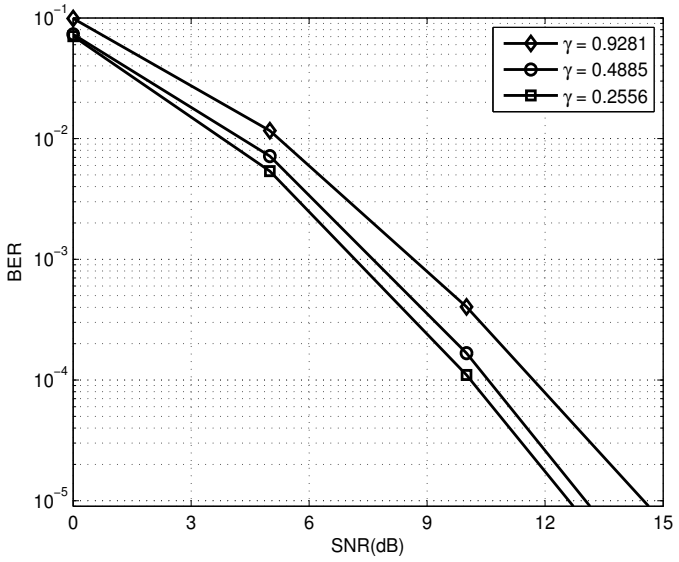

Fig. 3: BER versus SNR for cases of using different values of correlation (γ) between antenna beam patterns, $N_t = 2$, $N_r = 4$, two beams patterns.

0.2556), compared to the highly correlated $\gamma = 0.9281$. The results above show the correlation impact. However, in realistic application there are many factors to take into account, e.g. channel conditions, pattern correlation and ICI mitigation.

B. ML Detection

In [18], as previously stated, ML detection is used. The output of the channel is

$$\mathbf{y} = \mathbf{H}\mathbf{x} \ + \ \mathbf{v}. \tag{1}$$

The objective of the detector is to estimate the antenna pattern and then de-map them to the information bits. Assuming all the weight vectors transmitted are equally likely, the optimal detection is given by the ML method

$$\widehat{j} = \arg\min_{j} \|\mathbf{y} - \mathbf{H}\mathbf{x}_j\|^2. \tag{2}$$

The ML detection of $\widehat{j}$ is performed by an exhaustive search across all possible $\mathbf{x}_j$ for the minimum Euclidean distance $\|\mathbf{y} - \mathbf{H}\mathbf{x}_j\|^2$. Then, the information block can be de-mapped.

The computational complexity of ML is $\mathcal{O}((N_t N_r)^2 L)$, where L denotes the size of the constellation points [29]. The complexity increases when L is large, which causes problems when ML based on ABPM is applied. Linear detectors such as zero-forcing (ZF) and minimum mean-square error (MMSE) are good solutions with low complexity. However, their BER performance is far worse than ML.

The ZF equaliser removes all inter-symbol interference (ISI), and is ideal when the channel is noiseless. However, when the channel is noisy, the ZF equaliser will amplify the noise greatly in the attempt to invert the channel completely. The MMSE equaliser, on the other hand, does not usually eliminate ISI completely but instead minimizes the total power of the noise and ISI components in the output.

C. Lattice Reduction

Recently, LR aided detectors have been used for MIMO systems to achieve performance with full diversity and low complexity. [22,23,30,31] show the results of LR improvements over linear detectors with only a small increase in complexity. Lattice is a set of discrete points representing integer linear combinations of linearly independent vectors, which are called basis. Given *n* linearly independent vectors $c_1, c_2, ..., c_n \in \mathbb{R}$, the lattice generated by them is defined as $\mathcal{L}(c_1, c_2, ..., c_n) = \{\Sigma_{i=1}^{n} s_i c_i | s_i \in \mathbb{Z}\}$. $c_1, c_2, ..., c_n$ are referred to as the basis of the lattice [32].

A lattice can be represented by many different basis. The main purpose of lattice reduction is to find a good basis for a given lattice. A basis is considered to be good when the basis vectors are close to orthogonal. Recently, these LR aided linear equalisers have been utilised for detection in MIMO systems. Taking the model in (1), $\mathbf{x} \in \mathbb{Z}$, $\mathbf{Hx}$ forms a lattice spanned by the columns of $\mathbf{H}$ [33]. Therefore, the estimate of $\mathbf{x}$ (based on the received signal $\mathbf{y}$) is the point on the lattice that is closest to $\mathbf{y}$. High estimation accuracy is achieved when the lattice basis is orthogonal or close to that. This does not affect the performance of the ML detector, since it performs the same without taking the channel conditions into account. However, when the ML detector is not used, the channel conditions are important and in consequence when this condition (orthogonality between lattice vectors) is not satisfied, the performance tends to degrade. To quantify the orthogonality of a matrix, the orthogonality deficiency (od) [34] for a matrix $\mathbf{H}$ is defined as

$$od(\boldsymbol{H}) = 1 - \frac{\det(\mathbf{H}^H \mathbf{H})}{\prod_{n=1}^{N_t} \|\mathbf{h}_n\|}, \tag{3}$$

where $\mathbf{h}_n$ is the *n*th column of the matrix $\mathbf{H}$. It is important to note that $0 \leq od(\mathbf{H}) \leq 1$. If $od(\mathbf{H}) = 1$, $\mathbf{H}$ is singular and when $od(\mathbf{H}) = 0$ all the columns of $\mathbf{H}$ are orthogonal. Generally, it is not possible to get $od(\mathbf{H}) = 0$. If $od(\mathbf{H})$ is close to "0", it is said that $\mathbf{H}$ is close to be orthogonal.

Therefore, if the matrix $\tilde{\mathbf{H}}$ represents a new basis for the same lattice spanned by the columns in $\mathbf{H}$ and is more orthogonal than $\mathbf{H}$, it is anticipated that the performance using linear equalisers should be closer to the performance of the ML detector. The new channel matrix $\tilde{\mathbf{H}}$ is obtained by the LR technique. Arjen Lenstra, Hendrik Lenstra and Laszlo Lovász introduced the LLL algorithm, as a polynomial-time lattice reduction. It was proposed in 1982 and has since then been used in fields such as computer algebra, cryptology and algorithmic number theory [35]. The original applications of LLL algorithm were to give polynomial time algorithms for factorizing polynomials, to find simultaneous rational approximations to real numbers and to solve the integer linear programming problem in fixed dimensions. The LLL is the most popular algorithm used in LR aided detectors because in spite of not guaranteeing that the optimal basis will be found, it guarantees finding a basis with a better value of *od*. The highest complexity in terms of number of arithmetic operations in attempting to find a new basis using the LLL algorithm is $\mathcal{O}(R^4)$, where R is the size of the basis [24]. In [24], the detailed LLL algorithm using MATLAB notation is given. δ is the parameter which controls the performance and complexity of the LLL algorithm, it is randomly selected from $(\frac{1}{2}, 1)$, to guarantee a firm basis reduction. However, the computational complexity increases with larger values of δ [31,36]. The fundamental principle, as previously stated, is to combine a lattice reduction approach with low complexity linear detectors to establish an effective channel matrix $\tilde{\mathbf{H}}$ via the unimodular matrix $\mathbf{T}$, which means that all the entries of $\mathbf{T}^{-1}$ or $\mathbf{T}$ are integers and the determinant of $\mathbf{T}$ is ± 1 or $\pm i$. Fig. 4 illustrates the block diagram of the LR-based detection scheme. The block 'LR' generates the unimodular matrix $\mathbf{T}$ and the new basis $\tilde{\mathbf{H}}$. The model in (1) is rewritten as

$$\mathbf{y} = \mathbf{H}\mathbf{T}\mathbf{T}^{-1}\mathbf{x} \; + \; \mathbf{v} = \tilde{\mathbf{H}}\mathbf{z} \; + \; \mathbf{v}, \tag{4}$$

where $\tilde{\mathbf{H}} = \mathbf{H}\mathbf{T}$ and $\mathbf{z} = \mathbf{T}^{-1}\mathbf{x}$. With the basis changed, the traditional detector is used to compensate for the new channel $\tilde{\mathbf{H}} = \mathbf{H}\mathbf{T}$ to produce the estimation of $\hat{\mathbf{z}}$, and $\hat{\mathbf{x}}$ can be estimated through $\hat{\mathbf{x}} = \mathbf{T}\hat{\mathbf{z}}$. In this way, the LR algorithm is used in the linear detection equaliser.

With this new system model, linear equalisers can be applied to the channel matrix $\tilde{\mathbf{H}}$ to estimate $\mathbf{z}$. When ZF and MMSE are applied to the received signal $\mathbf{y}$ [22–25], we obtain

$$\hat{\mathbf{z}}_{_{ZF}} = \mathcal{Q}((\tilde{\mathbf{H}}^{H}\tilde{\mathbf{H}})^{-1}\tilde{\mathbf{H}}^{H}\mathbf{y}), \tag{5}$$

$$\hat{\mathbf{z}}_{_{MMSE}} = \mathcal{Q}((\tilde{\mathbf{H}}^{H}\tilde{\mathbf{H}} \; + \; \sigma_v^2\mathbf{T}^{H}\mathbf{T})^{-1}\tilde{\mathbf{H}}^{H}\mathbf{y}), \tag{6}$$

where $\mathcal{Q}(\cdot)$ means the quantisation operation. Thus, the estimate $\hat{\mathbf{x}}$ can be calculated as

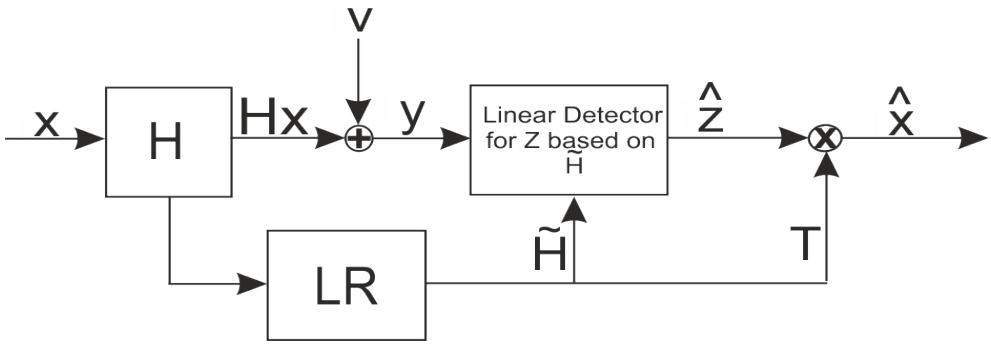

Fig. 4: Block diagram of LR method in combination with linear detection equaliser for MIMO system.

$$\hat{\mathbf{x}} = \mathbf{T}\hat{\mathbf{z}}. \tag{7}$$

It is known that $\hat{\mathbf{x}}$ contains both the weight vector and the symbol information. Thus, $\hat{\mathbf{w}}$ is estimated as the weight vector which has the highest correlation with the transmitted vector $\hat{\mathbf{x}}$

$$\widehat{\mathbf{w}} = \arg\max_{\ell} \|\mathbf{w}_{\ell}\hat{\mathbf{x}}\|^2, \tag{8}$$

where $\ell \in \{1, ..., 2^m\}$. The second block of data is estimated based on the estimation of the first block and the channel matrix, the detection of $\hat{s}$ is calculated as

$$\hat{s} = (\mathbf{H}\hat{\mathbf{w}})^{-1}\mathbf{y}. \tag{9}$$

As was explained, the estimation of the antenna weight vector is critical since it directly affects the symbols estimation. Therefore, as the ABPM symbol detection is obtained in two steps, an error on the antenna weight vector will be propagated to the APM symbol detection.

III. Performance Analysis

The ABPM scheme has been described as hybrid modulation due to its combination of antenna pattern with conventional APM schemes [18]. The ABPM transmission design changes based on the number of N_t and beam patterns, i.e. different design for different scenario. Thus, it is not possible to derive of an exact BER probability equation. For this reason, we derive a tight upper bound on the BER to validate and analyse the performance of ABPM. The pairwise error probability (PEP) of an ML detector is given by

$$
\begin{aligned}
&P\left(\mathbf{x}_j \to \mathbf{x}_{\hat{j}}\right) \\
&\quad = \mathbf{P}\Big(\left[\| \mathbf{y} - \mathbf{H}\mathbf{x}_{\hat{j}} \|^2 - \| \mathbf{y} - \mathbf{H}\mathbf{x}_j \|^2 \right] \le 0 \Big) \\
&\quad = \mathbf{P}\Big(\left[\| \mathbf{H}\left(\mathbf{x}_j - \mathbf{x}_{\hat{j}}\right) + \mathbf{v} \|^2 - \| \mathbf{v} \|^2 \right] \le 0 \Big) \\
&\quad = \mathbf{E}\left[Q\left(\sqrt{\frac{1}{2N_0} \sum_j \sum_{\hat{j}} \| \mathbf{H}\left(\mathbf{x}_j - \mathbf{x}_{\hat{j}}\right) \|^2} \right) \right].
\end{aligned}
\tag{10}
$$

Using the union bounding technique presented in [37], the BER of ABPM is union bounded as

$$
\begin{aligned}
P_{e,bit} &\le \mathbf{E}_{\mathbf{x}_j}\left[\sum_{\hat{j}} N(j,\hat{j}) P(\mathbf{x}_j \to \mathbf{x}_{\hat{j}}) \right] \\
&\le \sum_{j}^{L} \sum_{\hat{j},\hat{j}\neq j}^{L} \frac{N(j,\hat{j})}{kL} P(\mathbf{x}_j \to \mathbf{x}_{\hat{j}}),
\end{aligned}
\tag{11}
$$

where k is the number of information bits carried by one ABPM symbol, j and $\hat{j}$ denote the indices of the transmitted and estimated symbols, $\mathbf{x}_j$ and $\mathbf{x}_{\hat{j}}$ respectively; $\mathbf{E}_{\mathbf{x}_j}$ is the mean value of $P(\mathbf{x}_j \to \mathbf{x}_{\hat{j}})$, $N(j,\hat{j})$ is the number of different bits between symbols $\mathbf{x}_j$ and $\mathbf{x}_{\hat{j}}$ and $P(\mathbf{x}_j \to \mathbf{x}_{\hat{j}})$ is the PEP of detecting $\mathbf{x}_{\hat{j}}$ for transmitted $\mathbf{x}_j$ [38], which is calculated as

$$
P(\mathbf{x}_j \to \mathbf{x}_{\hat{j}}) = \left(\frac{1 - \frac{1}{u}}{2} \right)^{\Lambda} \sum_{n=0}^{\Lambda-1} 2^{-n} \binom{\Lambda - 1 + n}{n} \left(1 + \frac{1}{u} \right)^{n},
\tag{12}
$$

where $u = \sqrt{1 + \frac{1}{\frac{\rho d(j,\hat{j})}{2+b}}}$, $\Lambda = N_t N_r$, b is the number of beams and $d(j,\hat{j})$ is the Euclidean distance between $\mathbf{x}_j$ and $\mathbf{x}_{\hat{j}}$.

As expected, a larger minimum $d(j,\hat{j})$ results in better performance, similar to other conventional modulation techniques. Substituting (12) into (11), the upper bound of the bit error probability for ABPM can be expressed as

$$
\begin{aligned}
P_{e,bit} \le &\sum_{j}^{L} \sum_{\hat{j},\hat{j}\neq j}^{L} \frac{N(j,\hat{j})}{kL} \left(\frac{1 - \frac{1}{u}}{2} \right)^{\Lambda} \\
&\sum_{n=0}^{\Lambda-1} 2^{-n} \binom{\Lambda - 1 + n}{n} \left(1 + \frac{1}{u} \right)^{n}.
\end{aligned}
\tag{13}
$$

Note that $PEP = 0$ implies no error in the detection of $\mathbf{x}_j$, this is only possible if *u* has the value "1" in (12). Therefore, the accuracy of the tight upper bound depends on if *u* is close to "1". The parameter *u* depends on the minimum Euclidean distance $d(j, \hat{j})$. With larger *d*, *u* is closer to "1". Then, as *d* and *b* are inversely related, if *b* increases, *d* decreases and it degrades the system performance.

The upper bound indicates that larger distance between transmit vectors leads to better performance. Therefore, it is desirable that the selected antenna beam patterns have low correlation.

IV. Simulation results

In this section, examples are presented in order to show the benefits achieved by ABPM. Monte Carlo simulations are performed, and are run for at least 10^6 channel realizations. A flat Rayleigh fading channel with AWGN is used and perfect CSIT is assumed for simulation purposes.

Fig. 5 shows the BER performance of ABPM under different detection schemes. It compares the optimal detector ML with high computational complexity, to an LR aided detector combined with MMSE as a linear detector with low computational complexity, for data rates of $\eta = 3$ and 4 bits/s/Hz. When $\eta = 3$ bits/s/Hz, two different beam patterns are used to carry QPSK, the angle difference between two main lobes is 60° to guarantee low correlation as explained in Section II. When $\eta = 4$ bits/s/Hz, it has four different patterns carrying QPSK, the minimum angle separation is 30° between the main beams $\gamma = 0.3536$ (Table I), which implies that the four AoDs used are 50°, 20°, -20° and -50°. All schemes given use the same number of transmitters $N_t = 2$ and receivers $N_r = 5$.

It should be noted that in the case of $\eta = 3$ bits/s/Hz, the LR-MMSE has a performance very close to that of the optimal ML detector. This is possible due to low correlation between the patterns used. However, in the case of $\eta = 4$ bits/s/Hz, we can see a bigger difference between the two methods (2 dB at $P_{e,bit} = 10^{-5}$). The reason for this is that the distance between transmit vectors when $M = 4$, is smaller than when the system is using only 2 patterns. Another factor that impacts the BER performance, is that the detection is made in two stages. If the estimation of the first stage (antenna beam pattern represented by weights) is wrong, this error is carried through to the second stage which degrades the system performance. An upper bound for each case is added when the ML detector is used. Increasing the number of beam patterns reduces the Euclidean distance. Then, the upper bound is fairly tight with larger Euclidean distance (two beam patterns) in comparison to that of the case of four beam patterns.

Fig. 6 depicts ABPM's performance using both optimal and suboptimal detections in comparison with SM [11], GSSK [12] and V-BLAST with LR aided MMSE equalisation [24] with targeted $\eta = 3$ bits/s/Hz and $N_r = 5$. Four different transmission techniques are investigated to compare with the proposed ABPM

which has QPSK modulation and two different antenna beam patterns resulting in 8 constellation points. The first one is SM with $N_t = 4$ antennas and BPSK modulation. The second is SM with $N_t = 2$ antennas and QPSK modulation (both result in $N_t \times M = 8$ constellation points). The third is GSSK with $N_t = 5$, with two active transmitters. All three schemes are based on optimal ML detection. The fourth transmission technique is V-BLAST-LR with $N_t = 3$, BPSK modulation and $\eta = 3$ bits/s/Hz.

ABPM's performance with ML detection and new antenna pattern design described in this article clearly outperforms other schemes as shown in Fig. 6, where gains of 3 dB when compared to SM 2x5 and GSSK, and more than 3.5 dB over SM 4x5 are observed at $P_{e,bit} = 10^{-5}$. It should be noted that the comparison between all schemes assumes identical transmission rate. To achieve the desired rate, SM is designed with different number of transmit antennas and modulation sizes as shown in Fig. 6. The complexity at the receiver side of these three schemes (SM, GSSK and ABPM-ML) is comparable because they all use the ML detector. As Fig. 6 shows, ABPM-LR (dashed line) presents gains over schemes based on SM at $P_{e,bit} = 10^{-5}$: around 2 dB over SM 2x5 and GSSK, 2.5 dB when compared to SM 4x5; even when the SM schemes are based on ML detection which has a higher complexity than the linear detection used in ABPM-LR.

In comparing ABPM-LR to V-BLAST, it can be observed that the BER performance of the two is almost the same at low values of SNR. At $P_{e,bit} = 10^{-5}$, V-BLAST has less than 1 dB gain over ABPM-LR. However, it should be noted that ABPM-LR uses less transmit antennas to achieve the same spectral efficiency as V-BLAST. The advantages of using fewer transmitters are decreased costs of RF chains, saving of physical space, reduced requirement on synchronisation and less interference between transmit antennas. The performance gain of the ABPM- ML can be attributed to the improvement of spectral efficiency using antenna beam patterns which permit higher transmission diversity by transmitting the same information at each antenna. As well, it can be noticed that the upper bound is relatively tight and support the ABPM simulation results.

Fig. 7 shows the comparison of ABPM and SM schemes with CSIT and CSIR. An exhausted study of SM is presented in [39,40], including an analysis of SM considering CSIT. Adaptive spatial modulation (ASM) [41] and optimal hybrid spatial modulation (OH-SM) [42] have explored the transceiver channel diversity through the use of CSIT to minimise the transmission rate. ASM utilises different modulation order for different channel conditions. OH-SM is an extension of ASM, which incorporates the transmission mode switching (TMS) to use different transmission modes. All the schemes have a data rate of $\eta = 3$ bits/s/Hz. ABPM achieves gain of 1.5 dB when compared to ASM and performance similar to that of OH-SM at $P_{e,bit} = 10^{-3}$. However, at low SNRs, ABPM outperforms OH-SM of 2 dB. In addition,

adaptive modulation and TMS require high computational complexity and the number of required bits for feedback is large, particularly at high spatial dimension [42]. The traditional SM curves are shown in Fig. 7 only as a reference. The upper bound is relatively tight and support the ABPM simulation results.

Fig. 8 illustrates ABPM's performance with different number of transmit and receive antennas. Examples are presented to evaluate ABPM's performance using the same data rate 3 bits/s/Hz with two different antenna beam patterns and QPSK modulation. We noticed that when $N_t \leq N_r$, ABPM has better performance with larger N_t and N_r, since this scheme exploits both diversity at the transmitter and receiver sides. However, it is also noticeable that when $N_t > N_r$, (such as $N_t = 3$, $N_r = 2$) the performance is obviously degraded comparing to $N_t = 2$, $N_r = 2$ scheme. This is because each element of the vector $\mathbf{w}$ is transmitted by one antenna and then multiplied with one APM symbol. This transmission process is similar to spatial multiplexing. Then, it is expected that the constraint $N_t \leq N_r$ must be satisfied to recover the signal at the receiver.

Fig. 9 illustrates the BER performance of ABPM with $N_t = 2$, $N_r = 5$ with two and four beam patterns carrying 4-QAM symbols in comparison with their upper bound, with spectral efficiencies of 3 and 4 bits/s/Hz respectively. The 4-QAM with 2 beam patterns outperforms the system using 4-QAM with 4 beam patterns. The ML detector is used to demodulate the ABPM symbols. From this observation, it is clear that increasing the number of patterns degrades the BER performance due to the fact that the minimum distance between transmit vectors is reduced when more beam patterns are introduced. The upper bound is presented in order to validate the results obtained by simulations as explained in section III. It can be noticed that in the case of ABPM with 2 beams, the upper bound is tighter than ABPM with 4 beams. The reason for this is because (13) depends on the number of beams and the Euclidean distance. Therefore, increasing the number of beams, the value of parameter u in (13) increases, which will impact the accuracy of the bound.

It has been demonstrated that LR in combination with linear detectors (e.g. ZF, MMSE, etc.) guarantees a performance similar to that of the optimal detector ML but with a lower computational complexity. Fig. 10 compares the complexity between ML, LR-MMSE and MMSE detectors. It has been shown that ML has higher computational complexity in comparison to LR-MMSE. The number of arithmetic operations are increased when the numbers of N_t and/or N_r increase. The computational complexity increment of LR-MMSE over MMSE is due to the calculation of the LLL algorithm to find the new basis and the inverse of $\mathbf{T}$. As previously mentioned, ABPM has shown that using an LR-MMSE detector reduces the computational complexity achieving almost the same BER performance as with an ML detector.

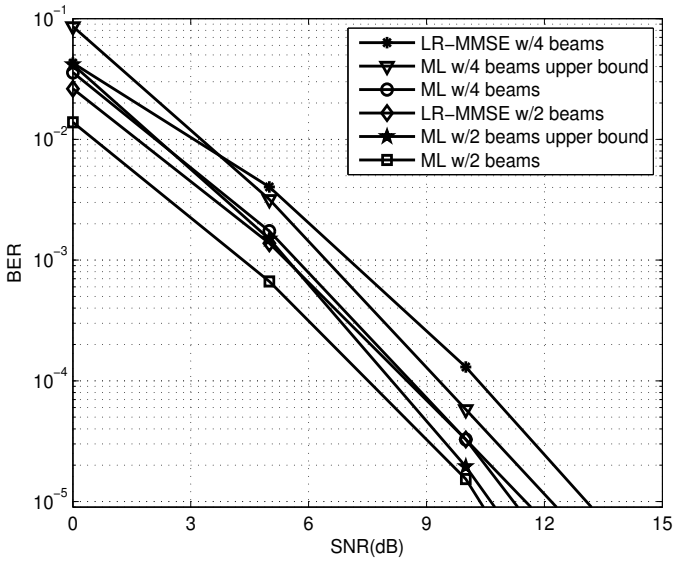

Fig. 5: BER performance versus SNR in comparison with ML and LR-MMSE detection for ABPM with $\eta = 3$ and 4 bits/s/Hz.

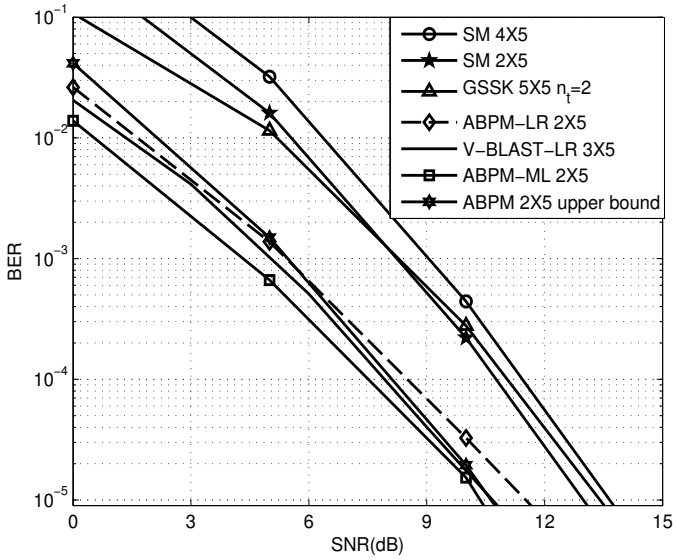

Fig. 6: BER comparison between ABPM with optimal and suboptimal detectors, spatial modulation and GSSK. To achieve $\eta = 3$ bits/s/Hz, ABPM uses two different transmission beam patterns and QPSK symbols, SM uses BPSK and QPSK symbols for $N_t = 4$ and $N_t = 2$, respectively. GSSK with $N_t = 5$ with $n_t = 2$ active transmitters and V-BLAST transmits BPSK symbols with $N_t = 3$. For all systems $N_r = 5$.

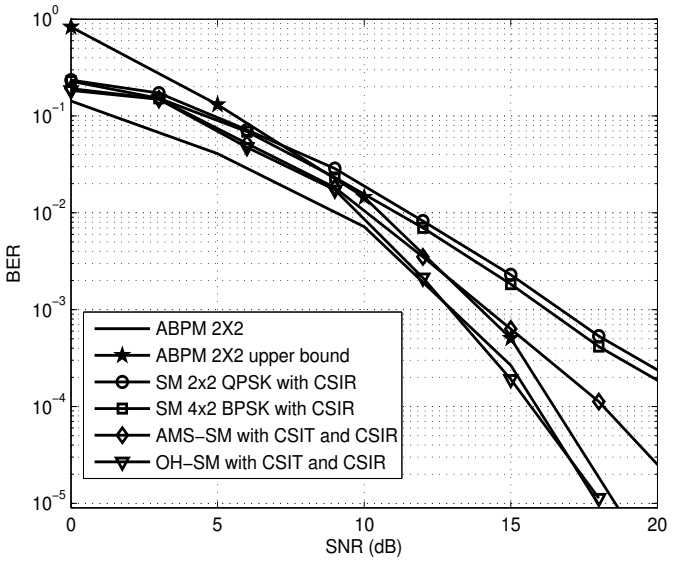

Fig. 7: BER versus SNR to compare ABPM and schemes based on SM considering CSIT and CSIR.

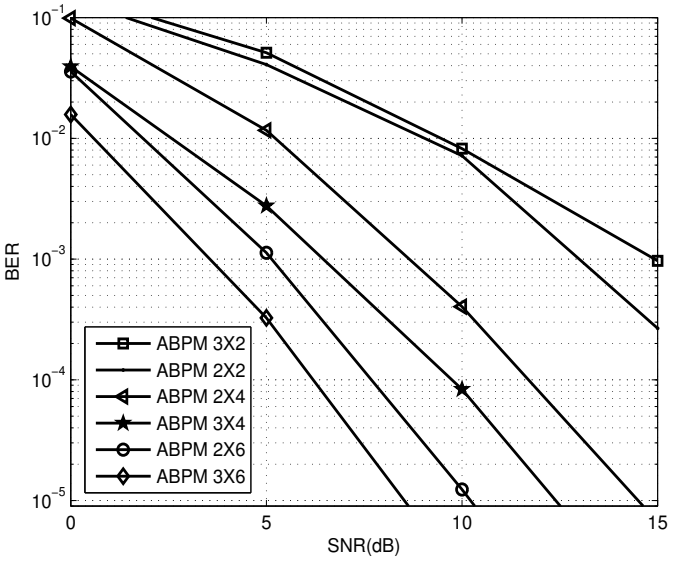

Fig. 8: Performance of ABPM with different MIMO scheme features (N_t and N_r), two different transmission beam patterns and QPSK symbols.

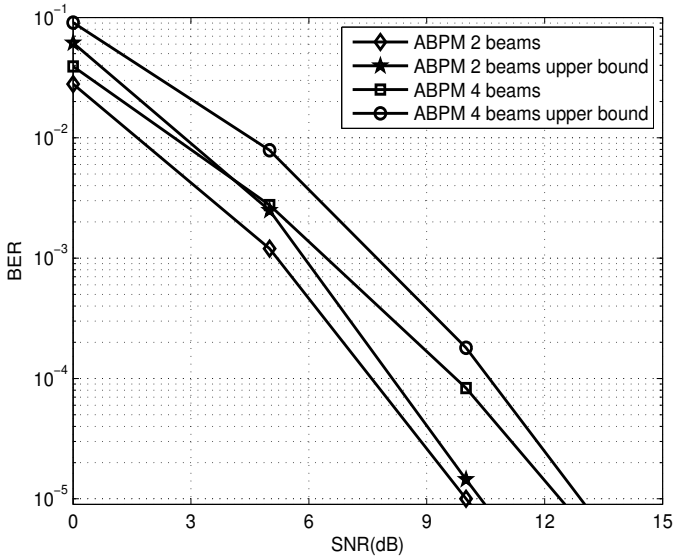

Fig. 9: BER versus SNR for 4-QAM modulation scheme with 2 and 4 beam patterns and their respective upper bounds.

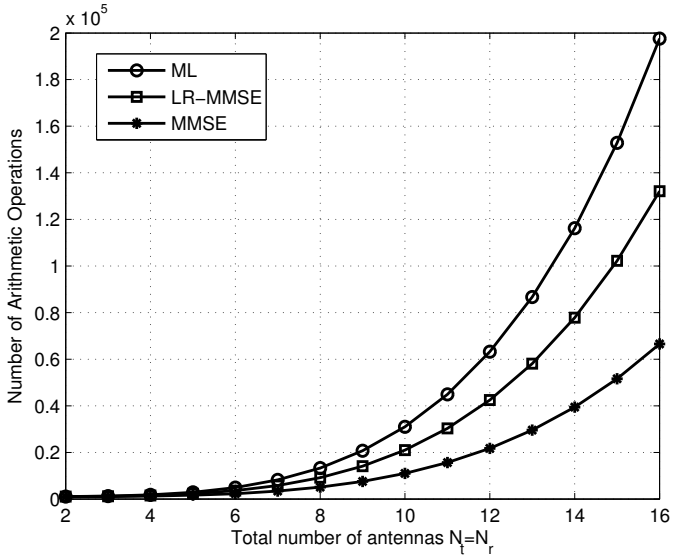

Fig. 10: Number of arithmetic operations of three different detectors.

V. CONCLUSION

A deeper study about the work done in [18] regarding transmission and detection design for the antenna beam pattern modulation (ABPM) has been presented. The antenna patterns are selected to minimise their correlation. A new LR-aided algorithm combined with MMSE is proposed as suboptimal detection to achieve performance which is similar to that of the optimal ML detector but with lower computational complexity. The BER results show that the ABPM-LR outperforms SM/ML and GSSK/ML by around 3 dB. An analytic upper bound has been derived to validate the simulation results. The antenna beam pattern modulation performance has indicated that it is a promising candidate for low complexity transmission techniques in future generations of communications systems such as in massive MIMO.

APPENDIX

Upper Bound Derivation

In this appendix we demonstrate the derivation of the upper bound for MIMO block fading channel. For coding systems, the PEP forms the basic structure for the union bound calculation of the error probability and is utilised as the main criteria for code design. The PEP between two arbitrary code-words **c** and **e** over N time slots in the Rayleigh fading channel [38] is expressed as

$$\begin{aligned} P(\mathbf{c} \rightarrow \mathbf{e}) = & \ 1 - \int_{R_m} p(\mathbf{c}|x)\mathrm{d}x \\ = & \ aE_w\left[Q\left(\sqrt{\sum_{j=1}^{N_t}\sum_{v=1}^{N_r} \mid w_j^v \mid^2}\right)\right] \end{aligned} \tag{A.14}$$

,

where R_m is the decision regions, $p(\mathbf{c}|x)$ is the joint probability density function (PDF), $a = \frac{E_s}{4N_tN_o}$, E_s is the symbol energy, N_o is Gaussian noise variance and $\mid w_j^v \mid$ is Rayleigh distributed.

Denote $w = w_1^1$ and $z_j^v = \frac{w_1^v}{w}$, $(j,v) \neq (1,1)$. Their joint PDF, $f(w, z_j^v \cdots z_{N_t}^{N_r})$ can be obtained from their cumulative density function $F(w, z_j^v \cdots z_{N_t}^{N_r})$ and expressed as

$$\begin{aligned} f(w, z_j^v \cdots z_{N_t}^{N_r}) = & \ w^{2N_tN_r-1}. \\ & \prod_{\substack{j=1 \\ (j,v)\neq(1,1)}}^{N_t}\prod_{v=1}^{N_r} z_j^v e^{-\frac{w^2}{2}\left(1+\sum_{j=1}^{N_t}\sum_{v=1}^{N_r}{}_{(j,v)\neq(1,1)}(z_j^v)^2\right)}. \end{aligned} \tag{A.15}$$

One of the properties of the complementary Gaussian cumulative distribution function (Q-function) is the integral property [43], which is expressed

$$\begin{aligned}\int_0^\infty x^{2n-1}\mathrm{e}^{-\frac{x^2}{2}}Q(\frac{x}{\sigma})\mathrm{d}x \\ &= \frac{(n-1)!}{2}(1-(\sigma^2+1)^{-\frac{1}{2}})^n \\ &\times \sum_{k=0}^{n-1} 2^{-k}\binom{n-1+k}{k}(1+(\sigma^2+1)^{-\frac{1}{2}})^k.\end{aligned} \tag{A.16}$$

Utilising (A.15) and (A.16), the PEP can be expressed as

$$P(\mathbf{c}\to\mathbf{e}) = \left(\frac{1-\frac{1}{u}}{2}\right)^{\Lambda}\sum_{k=0}^{\Lambda-1}2^{-k}\binom{\Lambda-1+k}{k}\left(1+\frac{1}{u}\right)^k, \tag{A.17}$$

where $u=\sqrt{1+\frac{1}{a}}$, $\Lambda = N_tN_r$.

REFERENCES

[1] S. Alamouti, "A simple transmit diversity technique for wireless communications," *IEEE J. Sel. Areas Commun.*, vol. 16, no. 8, pp. 1451–1458, 1998.

[2] V. Tarokh, N. Seshadri, and A. Calderbank, "Space-time codes for high data rate wireless communication: Performance criterion and code construction," *IEEE Trans. Inf. Theory*, vol. 44, no. 2, pp. 1185–1191, 1998.

[3] P. Wolniansky, G. Foschini, G. Golden, and R. Valenzuela, "V-BLAST: An architecture for realizing very high data rates over the rich-scattering wireless channel," in *URSI Int. Symp. Signals, Syst. and Electron. (ISSSE) 1998*. IEEE, 1998, pp. 295–300.

[4] L. Zheng and D. Tse, "Diversity and multiplexing: A fundamental tradeoff in multiple-antenna channels," *IEEE Tran. Inf. Theory*, vol. 49, no. 5, pp. 1073–1096, 2003.

[5] V. Tarokh, A. Naguib, N. Seshadri, and A. Calderbank, "Combined array processing and space-time coding," *IEEE Trans. Inf. Theory*, vol. 45, no. 4, pp. 1121–1128, 1999.

[6] M. Chiani, M. Z. Win, and A. Zanella, "On the capacity of spatially correlated MIMO Rayleigh-fading channels," *IEEE Trans. Inf. Theory*, vol. 49, no. 10, pp. 2363–2371, 2003.

[7] M. O. Damen, A. Abdi, and M. Kaveh, "On the effect of correlated fading on several space-time coding and detection schemes," in *54th Veh. Technol. Conf. (VTC) 2001 Fall*, vol. 1. IEEE, 2001, pp. 13–16.

[8] R. Mesleh, H. Haas, C. Ahn, and S. Yun, "Spatial modulation: A new low complexity spectral efficiency enhancing technique," in *1st Int. Conf. Commun. and Network. (ChinaCom) 2006*, 2006, pp. 1–5.

[9] R. Mesleh, H. Haas, S. Sinanovic, C. Ahn, and S. Yun, "Spatial modulation," *IEEE Trans. Veh. Technol.*, vol. 57, no. 4, pp. 2228–2241, 2008.

[10] A. ElKalagy and E. AlSusa, "A novel two-antenna spatial modulation technique with simultaneous transmission," in *17th Int. Conf. Softw. Telecommun. Comput. Networks (SoftCOM) 2009*, sept. 2009, pp. 230 –234.

[11] J. Jeganathan, A. Ghrayeb, and L. Szczecinski, "Spatial modulation: optimal detection and performance analysis," *IEEE Commun. Lett.*, vol. 12, no. 8, pp. 545–547, 2008.

[12] ——, "Generalized space shift keying modulation for MIMO channels," in *IEEE 19th Int. Symp. Pers., Ind. and Mobile Radio Commun. (PIMRC) 2008*, 2008, pp. 1–5.

[13] A. Younis, N. Serafimovski, R. Mesleh, and H. Haas, "Generalised spatial modulation," in *44th Conf. Signals, Syst. and Comput. (ASILOMAR) 2010*. IEEE, pp. 1498–1502.

[14] R. Ramirez-Gutierrez, L. Zhang, J. Elmirghani, and R. Fa, "Generalized Phase Spatial Shift Keying Modulation for MIMO Channels," in *73rd Veh. Technol. Conf. (VTC Spring) 2011*, may 2011, pp. 1 –5.

[15] A. Kalis, A. G. Kanatas, and C. B. Papadias, "A novel approach to MIMO transmission using a single RF front end," *IEEE J. Sel. Areas Commun.*, vol. 26, no. 6, pp. 972–980, 2008.

[16] O. N. Alrabadi, C. B. Papadias, A. Kalis, and R. Prasad, "A universal encoding scheme for MIMO transmission using a single active element for PSK modulation schemes," *IEEE Trans. Wireless Commun.*, vol. 8, no. 10, pp. 5133–5142, 2009.

[17] K. Antonis, C. Papadias, and A. Kanatas, "An ESPAR Antenna for Beamspace-MIMO Systems Using PSK Modulation Schemes," in *IEEE Int. Conf. Commun. (ICC) 2007*, june 2007, pp. 5348 –5353.

[18] R. Ramirez-Gutierrez, L. Zhang, J. Elmirghani, and A. Almutairi, "Antenna Beam Pattern Modulation for MIMO Channels," in *8th Int. Wireless Commun. and Mobile Comput. Conf. (IWCMC) 2012*. IEEE, 2012, pp. 591–595.

[19] Y. Jiang, M. Varanasi, and J. Li, "Performance analysis of ZF and MMSE equalizers for MIMO systems: an in-depth study of the high SNR regime," vol. 57, no. 4. IEEE, 2011, pp. 2008–2026.

[20] J. Cassels, *An introduction to the geometry of numbers*. Springer Verlag, 1997.

[21] J. Niu and I. Lu, "A new lattice-reduction-based receiver for MIMO systems," in *41st Annu. Conf. Inf. Sci. and Syst. (CISS) 2007*. IEEE, 2007, pp. 499–504.

[22] D. Wubben, R. Bohnke, V. Kuhn, and K. Kammeyer, "Near-maximum-likelihood detection of MIMO systems using MMSE-based lattice reduction," in *IEEE Int. Conf. Commun.*, vol. 2. IEEE, 2004, pp. 798–802.

[23] H. Yao and G. Wornell, "Lattice-reduction-aided detectors for MIMO communication systems," in *IEEE Global Telecommun. Conf. (GLOBECOM) 2002*, vol. 1. IEEE, 2002, pp. 424–428.

[24] X. Ma and W. Zhang, "Performance analysis for MIMO systems with lattice-reduction aided linear equalization," *IEEE Trans. Commun.*, vol. 56, no. 2, pp. 309–318, 2008.

[25] Y. Gan, C. Ling, and W. Mow, "Complex lattice reduction algorithm for low-complexity full-diversity MIMO detection," *IEEE Trans. Signal Process.*, vol. 57, no. 7, pp. 2701–2710, 2009.

[26] A. Lenstra, H. Lenstra, and L. Lovász, "Factoring polynomials with rational coefficients," *Mathematische Annalen*, vol. 261, no. 4, pp. 515–534, 1982.

[27] J. Hoydis, S. Ten Brink, and M. Debbah, "Massive MIMO: How many antennas do we need?" in *49th Annu. Allerton Conf. Commun., Control and Comput.* IEEE, 2011, pp. 545–550.

[28] J. Andrews, A. Ghosh, and R. Muhamed, *Fundamentals of WiMAX: understanding broadband wireless networking*. Prentice Hall PTR, 2007.

[29] M. Leng and Y.-C. Wu, "Low-complexity maximum-likelihood estimator for clock synchronization of wireless sensor nodes under exponential delays," *IEEE Trans. Signal Process.*, vol. 59, no. 10, pp. 4860–4870, 2011.

[30] C. Windpassinger and R. F. Fischer, "Low-complexity near-maximum-likelihood detection and precoding for MIMO systems using lattice reduction," in *Proc. Inf. Theory Workshop*. IEEE, 2003, pp. 345–348.

[31] D. Wubben, R. Bohnke, V. Kuhn, and K.-D. Kammeyer, "MMSE extension of V-BLAST based on sorted QR decomposition," in *58th Veh. Technol. Conf. (VTC) 2003-Fall*, vol. 1. IEEE, 2003, pp. 508–512.

[32] F. T. Luk, S. Qiao, and W. Zhang, "A lattice basis reduction algorithm," *Institute for Computational Mathematics Technical Report 10*, vol. 4, 2010.

[33] E. Agrell, T. Eriksson, A. Vardy, and K. Zeger, "Closest point search in lattices," *IEEE Trans. Inf. Theory*, vol. 48, no. 8, pp. 2201–2214, 2002.

[34] M. Taherzadeh, A. Mobasher, and A. Khandani, "Lattice-basis reduction achieves the precoding diversity in MIMO broadcast systems," in *39th Conf. Inf. Sci. and Syst. (CISS) 2005*, 2005.

[35] P. Q. Nguyen and B. Valle, *The LLL algorithm: survey and applications*. Springer Publishing Company, Incorporated, 2009.

[36] Q. Zhou and X. Ma, "Element-Based Lattice Reduction Algorithms for Large MIMO Detection," *IEEE J. Sel. Areas Commun.*, vol. 31, no. 2, pp. 274–286, 2013.

[37] J. Proakis and M. Salehi, *Digital communications*. McGraw-hill New York, 2001, pp. 261–262.

[38] Z. Lin, E. Erkip, and A. Stefanov, "The exact pairwise error probability for MIMO block fading channel," in *Proc. Int. Symp. Inf. Theory Appl.* Citeseer, 2004, pp. 728–732.

[39] M. Di Renzo, H. Haas, A. Ghrayeb, S. Sugiura, and L. Hanzo, "Spatial modulation for generalized MIMO: challenges, opportunities, and implementation," *IEEE Proc.*, vol. 102, no. 1, pp. 56–103, 2014.

[40] M. Di Renzo, H. Haas, A. Ghrayeb *et al.*, "Spatial modulation for MIMO wireless systems," in *IEEE Wireless Commun. Network Conf. WCNC 2013*, 2013.

[41] P. Yang, Y. Xiao, Y. Yu, and S. Li, "Adaptive spatial modulation for wireless MIMO transmission systems," *IEEE Commun. Lett.*, vol. 15, no. 6, pp. 602–604, 2011.

[42] P. Yang, Y. Xiao, L. Li, Q. Tang, Y. Yu, and S. Li, "Link adaptation for spatial modulation with limited feedback," *IEEE Trans. Veh. Technol.*, vol. 61, no. 8, pp. 3808–3813, 2012.

[43] S. Verdu, *Multiuser Detection*. Cambridge University Press, 1998.